Combined EEG-fMRI and ESI improves localisation of paediatric focal epilepsy

Maria Centeno, MD, PhD[1,2], Tim M. Tierney, PhD[1], Suejen Perani, PhD[1,3], Elhum A. Shamshiri, BA[1], Kelly StPier[2], Charlotte Wilkinson[2], Daniel Konn, MD, PhD[4], Serge Vulliemoz, MD, PhD[5], Frédéric Grouiller, PhD[6], Louis Lemieux, PhD[7], Ronit M. Pressler, MD, PhD[8,9], Christopher A. Clark, PhD[1], J. Helen Cross, MD, FRCP, FRCPCH[8,9], David W Carmichael, PhD[1]

[1] *Developmental Imaging and Biophysics Section. UCL Great Ormond Street Institute of Child Health. University College London. London, UK*
[2] *Epilepsy Unit, Department of Neurophysiology, Great Ormond Street Hospital, London, UK*
[3] *Division of Neuroscience. Institute of Psychiatry, Psychology & Neuroscience. King's College London. London, UK*
[4] *Neurophysiology Department. University Hospital Southampton. Southampton, UK*
[5] *EEG and Epilepsy Unit, Neurology, University Hospitals and Faculty of Medicine of Geneva. Switzerland*
[6] *Swiss Center for Affective Sciences, University of Geneva, Geneva, Switzerland*
[7] *Department of Clinical and Experimental epilepsy. Institute of Neurology. University College London. London, UK*
[8] *Neuroscience Medicine, Great Ormond Street Hospital for Children, London, UK*
[9] *Clinical Neuroscience, UCL Great Ormond Street Institute of Child Health, London, UK*

Corresponding author: Maria Centeno
Corresponding author's address: Developmental Imaging and Biophysics Section. UCL Great Ormond Street Institute of Child Health. 30 Guilford Street. WC1N 1EH London UK
Corresponding author's phone and fax: +44 (0) 7984547883 / +44 (0) 2079052358
Corresponding author's e-mail address: m.centeno@ucl.ac.uk

Running head: Combined EEG-fMRI & ESI predicts surgery outcome in epilepsy
Number of words in abstract: 246
Number of words in main text: 4341
Number of figures: 3
Number of tables: 1
Number of supplementary tables: 2

This article has been accepted for publication and undergone full peer review but has not been through the copyediting, typesetting, pagination and proofreading process which may lead to differences between this version and the Version of Record. Please cite this article as an 'Accepted Article', doi: 10.1002/ana.25003

ABSTRACT

Objective

Surgical treatment in epilepsy is effective if the epileptogenic zone (EZ) can be correctly localized and characterized. Here we use simultaneous Electroencephalography-functional MRI (EEG-fMRI) data to derive EEG-fMRI and Electrical Source Imaging (ESI) maps. Their yield and their individual and combined ability to 1) localize the epileptogenic zone and 2) predict seizure outcome was then evaluated.

Methods

Fifty-three children with drug-resistant epilepsy underwent EEG-fMRI. Interictal discharges were mapped using both EEG-fMRI haemodynamic responses and Electrical Source Imaging (ESI). A single localization was derived from each individual test (EEG-fMRI global maxima (GM)/ESI maxima) and from the combination of both maps (EEG-fMRI/ESI spatial intersection). To determine the localisation accuracy and its predictive performance the individual and combined test localisations were compared to the presumed EZ and to the postsurgical outcome.

Results

Fifty-two/53 patients had significant maps; 47/53 for EEG-fMRI; 44/53 for ESI; 34/53 had both. The epileptogenic zone was well characterised in 29 patients; 26 had an EEG-fMRI GM localisation which was correct in 11; 22 patients had ESI localisation which was correct in 17; 12 patients had combined EEG-fMRI and ESI which was correct in 11.

Seizure outcome following resection was correctly predicted by EEG-fMRI GM in 8/20 patients, by the ESI maxima in 13/16. The combined EEG-fMRI/ESI region entirely predicted outcome in 9/9 patients including 3 with no lesion visible on MRI.

Interpretation

EEG-fMRI combined with ESI provides a simple unbiased localisation that may predict surgery better than each individual test including in MRI-negative patients.

INTRODUCTION

Paediatric epilepsy surgery has become increasingly important due to the potential benefits of earlier surgery to optimise seizure and cognitive outcome [1]. In this patient group non-invasive techniques able to localize the epileptogenic zone (EZ) with good sensitivity and specificity are particularly desirable, specifically in patients without an MRI visible lesion. EEG-fMRI and ESI are both good candidates but definitive studies are needed to determine their diagnostic performance in the paediatric population.

Previous EEG-fMRI studies in adults have shown that fMRI can map the epileptogenic zone using interictal [2, 3] and ictal [4] events. Compared to clinical EEG alone, EEG-fMRI has been shown to provide a more accurate localisation of the epileptogenic zone (EZ) in up to 2/3 of the cases [5],to have a good degree of correlation with invasive EEG findings [6], and to be predictive of good surgical outcome [7, 8]. However, EEG-fMRI maps often show multiple regions of activity which, while being consistent with the idea that epilepsy is a network disease [9, 10 6, 11, 12], complicates interpretation where a single spatial target is typically required for surgery to proceed. Previous studies have often used the statistic global maxima (GM) [8, 13], or have constrained the search area to the spike field [5] or to the clinically defined epileptic focus [2, 3] to obtain a localisation. Unfortunately, these approaches can have low sensitivity (in the case of GM) or are dependent on subjective interpretation if using a clinically defined focus or are based on the interictal epileptiform discharges (IED) field. Furthermore, in a paediatric cohort clinical EEG is often less localizing, repeat surgery relatively common and therefore the use of IED fields maybe problematic. Recently EEG-fMRI was shown to be feasible in children from 6-18 years old without sedation and possibly have a higher yield compared with adults in a selected population[14] . Additionally, new methodological developments (topographic voltage correlation analysis)[15] allow EEG-fMRI maps to be obtained without IEDs.

ESI has been shown to localize the EZ with high sensitivity and specificity in a mixed group of adults and children using high density (>32 channel) EEG [16] and shown promise in a paediatric cohort [17]. ESI can have limitations in cases of deep sources [18], previous surgery [19] or where IEDs are not typical discrete events and it has a limited spatial accuracy. Studies have investigated the spatial consistency of EEG-fMRI and ESI maps [20, 21] and their localisation performance [22] but they have not been combined to improve their potential predictive value.

Here, high-density EEG-fMRI data was used to derive ESI and EEG-fMRI maps. We aimed to: a) quantify the yield; b) determine the localizing value; and c) asses the predictive value of EEG-fMRI and ESI individually and as combined test in the largest paediatric focal epilepsy population studied to date with either method.

METHODS

Subjects

Fifty-three children with drug-resistant epilepsy underwent simultaneous EEG-fMRI. At the point of recruitment, the children were undergoing evaluation for resective epilepsy surgery at Great Ormond Street Hospital for Children (London, UK). The patients were recruited prospectively between November 2011 and May 2015; inclusion criteria for the study were the presence of frequent interictal discharges and the capacity to undergo an unsedated MRI.

The clinical data of the 53 patients are summarized in supplementary Table 1. Thirty patients had a structural lesion on MRI (56%) and twenty-three (44%) were lesion negative.

a) Patient group for yield assessment

All 53 patients were included in the calculation of test yield.

b) Patient group for localisation value assessment

All patients underwent videotelemetry-EEG to document seizures and structural MRI for pre-surgical assessment. In 29/53 patients the EZ was considered well-localised based on the following criteria: 1) MRI lesion concordant with the electro-clinical data (15 patients) or 2) good outcome following surgery (14 patients; 12 lesional/2 non-lesional). Patients with a poor outcome or without an MRI lesion (unless they had a good surgical outcome) were excluded from this group because their EZ was not well localised. The volume of the EZ was estimated and these values are included in supplementary Table 1.

c) Patient group for prediction of surgical outcome assessment

All 20 patients within the study who underwent resective surgery were included. Five out of 20 had normal MRI. Surgical outcome for each patient was classified according to the modified ILAE classification system [23] before being further divided into good or poor outcome based on the surgical goal being met. Good outcomes were therefore considered to be ILAE class 1 and 2. In 3 patients with large lesions (involving more than one lobe) a partial resection of the lesion was chosen in order to spare eloquent cortex. In these patients if a significant seizure reduction of >50% was achieved (ILAE class 4) the outcome was considered to be a favourable as this was the a priori surgical aim. For all other categories outcome was considered to be poor. The relative brain volume that was resected was estimated and these values are included in supplementary Table 1.

EEG-fMRI acquisition

Full scanning protocol details are described in our previous work [14]. Patients were prepared with a 64-electrodes MRI compatible EEG cap (Easy cap, Brain Products, Munich, Germany). All patients underwent between 2 to 4 EEG-fMRI sessions lasting 10 minutes each (300

volumes TR 2.16s) and a T1-weighted whole-brain structural image. In order to keep consistency across subjects only the first two sessions (20 minutes) of EEG-fMRI were used in the analysis with the added benefit of reduced subject movement without affecting BOLD results[14]. In 2 patients in whom seizures with movement occurred during the first 2 sessions the subsequent sessions free of seizures were analysed.

Pre-processing of EEG and identification/classification of interictal epileptiform discharges (IED) on EEG traces were carried out as described previously in Centeno et al. [14]. In summary, IED for each subject were classified as a separate IED type according to the topographical distribution of the activity[13].

EEG-fMRI analysis

IED-correlation analysis

A mass univariate fMRI analysis was performed using SPM8 version r5232 (http://www.spm.fil.ion.ucl.ac.uk) running in matlab (Mathworks, Natick, USA).

Pre-processing consisted of image realignment (SPM8) followed by the removal of non-physiological signal changes using FIACH [24]. Slice time correction and smoothing with an 8mm kernel was subsequently applied (SPM8).

A general linear model was generated for each subject where for each IED type, IED onset (and duration in the case of IED runs) was convolved with the canonical HRF and its time and dispersion derivatives. Motion realignment parameters and FIACH physiological noise regressors [14, 24] were entered as effects of no interest. Brain regions with signal changes associated with each IED type were tested with an F-test across the three IED regressors (HRF and the two derivatives) to account for variability in the haemodynamic response shape [25, 26]. A more detailed explanation of the model used can be found in Centeno et al. [14].

Topographic IED voltage map correlation

In those patients in whom IED were not captured during the EEG-fMRI sessions, a regression analysis of the typical IED topographic voltage maps was applied to the EEG-fMRI data following the procedure described by Grouiller et al [15]. In brief, a patient's IED topography derived from their clinical EEG is spatially correlated with the topography of the EEG obtained inside the scanner at each time point. The fMRI signal changes associated with an increased correlation to the IED topography are obtained, which can reflect the generators of focal epileptic activity [27, 28].

Changes in Blood Oxygenation Level Dependant (BOLD) fMRI signal were considered significant at an individual level above a threshold of $p<0.001$ (uncorrected) and a cluster size voxel with a minimum of 5 contiguous voxels[14]. This threshold is arbitrary but was chosen apriori to strike an appropriate balance between sensitivity and specificity based on

the range of design efficiency that is encountered between patients. This threshold was applied to both IED-related and topographic correlation analysis maps.

Electrical source imaging

Only patients with IEDs captured during the EEG-fMRI sessions (using a 64 electrode cap) had electrical source imaging (ESI). We calculated the ESI of each IED type identified on the EEG using Cartool software (https://sites.google.com/site/fbmlab/cartool) and followed the procedure described in Vulliemoz et al. [29].

Localisation derived from EEG-fMRI and ESI individually and combined

A single localisation was derived from each EEG-fMRI and ESI map used individually and then subsequently a combined localisation was derived (Fig 1).

Individual test localisation

The single localisation obtained from EEG-fMRI maps was the cluster containing the statistical global maximum. The single localisation from the ESI maps was the ESI maxima solution point for the map corresponding to the 50% rising phase of the IED.

Combined EEG-fMRI/ESI localisation

To obtain a single localisation from the combination of EEG-fMRI and ESI, both maps were coregistered and overlaid on the subject's structural T1-wighted image. Combined EEG-fMRI/ESI localisation was extracted in those cases in whom ESI maxima and an EEG-fMRI cluster were localised to the same sublobar region. Sublobar regions were defined as follows[30] : frontal polar, dorsal lateral frontal, mesial frontal, lateral parietal, mesial parietal, lateral occipital, mesial occipital, lateral temporal, temporal polar, and mesial temporal. The location derived from the combined EEG-fMRI and ESI maps was defined as the region that comprised both the ESI maxima and the nearest EEG-fMRI cluster within the same sublobe. Additionally, the Euclidian distance between the ESI maxima and EEG-fMRI cluster located in the same sublobe was calculated for the combined EEG-fMRI/ESI cases.

Assessment of the value of the EEG-fMRI and ESI

a) Test yield

To determine the ability of the test to provide a localisation result the 'test yield' was calculated and is given by the number of patients with a test localisation result/total number that received the test.

b) Localisation accuracy

Here, we aimed to address the question 'given a test localisation result, what is the probability that it is correct?'. To do this, the patient group with a well localised EZ (n=29

see above) was used (Fig 2). When the test resulted in a localisation and it fell within the EZ it was classed as a true positive (a correct localisation); otherwise if the test resulted in a localisation and it did not fall within the EZ it was considered a false positive (an incorrect localisation). This was repeated for the individual localisation results from ESI and EEG-fMRI and for the combined localisation. Note that where the test does not provide a localisation, the test cannot be categorised as providing true or false, positive or negative localisation information (the absence of evidence cannot be taken as evidence of absence).

c) Surgery outcome prediction

Thirdly we aimed to assess the ability of EEG-fMRI and ESI localisation to predict seizure outcome (Fig 2). In patients who underwent surgery, we defined a true positive as being when the localisation provided by the test was resected with a good outcome; false positive as when the localisation provided by the test was resected followed by a poor outcome. True and false negatives were defined as the localisation provided by the test not being resected and the outcome being poor and good respectively[8]. True positives and true negatives were considered correct predictions (prediction successes), otherwise the prediction was incorrect (prediction failures).

Statistical analysis and confidence estimates

Binomial calculations are often used to quantify uncertainty in diagnostic test sensitivities using confidence intervals. However, these intervals are inaccurate if percentages approach 100%. We therefore adopted a Bayesian approach to estimating the sensitivity and the associated uncertainty. The prior information we incorporate is in the form of a Beta distribution which is the typical prior for proportions [31]. The Beta distribution has two parameters: α and β which both have a meaningful clinical interpretation. For EZ localisation, the parameter α is simply the number of times a given test correctly localised the EZ. Whereas the β parameter is the number of times the test incorrectly localised the EZ. For surgical prediction α is the number of successful predictions (true positives plus true negatives) whereas β is the number of failures (false positives plus false negatives).

The values for α and β for the prior distribution can incorporate information from previous studies. When none is available the starting assumption is that α *and* β are equally likely and so α=β=1 (in this special case the prior is a uniform distribution also called a flat prior). For EEG-fMRI-GM we incorporated information from two studies [8, 13]. The resulting prior for EEG-FMRI-GM sensitivity(θ) was $\theta \sim \beta eta(14,10)$. For ESI we used the study by Brodbeck et al[16]. The resulting prior for ESI is $\theta \sim \beta eta(45,9)$. In the absence of data for the combined method the prior remained uninformative ($\theta \sim \beta eta(1,1)$).This prior remained the same for the localisation sensitivity and the prediction of surgical outcome. These priors were then used together with our data to describe the posterior distribution of sensitivity in the population. The uncertainty was then simply characterised using a 95% credible interval calculated using the 0.975 and 0.025 quantiles of the posterior distribution.

The chance level of localisation was based on the estimated EZ volume or resection volume (see supplementary Table 1). The distribution of this variable was unknown a priori. In order to calculate the mean chance level of localisation and associated measures of uncertainty we therefore used a bootstrap procedure. This was implemented in the boot package of the R Programming language[32, 33]. The number of bootstrap replicates was 5000. Credible intervals were calculated using the 0.975 and 0.025 quantiles of the resulting distribution of the mean. The sensitivity of a given test lies within the credible interval with 95% probability and is therefore considered here to be significantly improved (relative to chance levels or other tests) when the 95% intervals did not overlap.

RESULTS

Forty-four out of 53 patients (83%) had IED during EEG-fMRI sessions. The number of IED types per patient ranged from 1 to 4 (mean 1.6). Twenty-four patients (54%) had 1 IED type; fourteen patients (31%) had 2 types of IED, five patients (11%) had 3 types of IED and one patient (2%) had 4 types of IED (supplementary Table 2). The results are summarised in Table 1.

a) Test Yield

In summary, 52/53 patients (98%) had a significant result for at least one of the tests.

Forty-seven/53 patients had significant clusters of activity on the EEG-fMRI maps (88% test yield). Thirty-nine of the EEG-fMRI maps were IED-related and eight were topographic-voltage-correlation maps (8/9 patients without IEDs). The EEG-fMRI maps contained more than one cluster in 46 out of 47 patients.

ESI was obtained in 39/53 patients (73% test yield). In fourteen patients ESI could not be obtained due to the following reasons: no IED (nine patients); IED rhythmic irregular bursts (one patient), EEG artefact (one patient), structural MRI pre-processing problems (three patients).

The combined ESI/EEG-fMRI gave a single localisation in 23/53 patients (43% test yield). In 11/23 patients, the EEG-fMRI cluster that was concordant with ESI was the global maxima. The mean distance between EEG-fMRI and ESI maxima was 14.6 mm ranging from 5 to 30 mm in the combined EEG-fMRI/ESI. A summary of test yield for MRI negative and lesional patients is shown in Figure 3. Details of individual subject's localisation derived from EEG-fMRI/ESI used individually and combined can be found in supplementary Table2.

b) Localisation accuracy

Twenty-six out of the 29 patients with a well characterized EZ had significant BOLD changes on EEG-fMRI maps; 11/26 correctly localised the EZ with the GM. Twenty-two patients out of the 29 had an ESI map; in 17/22 the maxima correctly localised the EZ. Twelve out of the

29 had a combined localisation from EEG-fMRI and ESI maps; 11/12 correctly localised the EZ (Table 1). The localisation performance of all tests was above chance levels. Both ESI and the combined test were better at localising than the EEG-fMRI GM method based on the criteria of non-overlapping 95% intervals (see table 1).

c) *Surgical prediction accuracy*

Twenty patients underwent surgery and had post-operative outcome (mean 29 months, range 10 to 57 months). Eleven patients (55%) were seizure free. Nine patients continued having seizures after surgery and were classified as ILAE class 2 (1 patient), class 4 (3 patients) and class 5 (5 patients) (see supplementary Table 1). Two of the patients underwent a partial resection of a large lesion with the aim of significantly reducing the seizure burden but not necessarily seizure freedom. These patients (#28 and #39) had an outcome ILAE 4, with a reduction >of 50% and so were additionally considered as having a good outcome based on the different aim of the surgery. Therefore, the total number of patients with good outcome was 14/20. Five patients in the surgical group were MRI negative (#2,#7,#25,#44,#50). Four of these had both EEG-fMRI and ESI maps with three of them having a combined EEG-fMRI/ESI localisation (#25,#44,#50).

Outcome was correctly predicted in 8/20 patients by the EEG-fMRI GM, in 13/16 by ESI and in 9/9 by combined EEG-fMRI and ESI. The predictive performance of all tests was above chance level, and both ESI and the combined test were better at localising than the EEG-fMRI GM methods based on the criteria of non-overlapping 95% intervals (see table 1)

DISCUSSION

In this study, we retrospectively evaluated the potential localising and predictive value of EEG-fMRI and ESI individually and when used as a combined test in the largest paediatric focal epilepsy population studied to date with either method.

The yield of EEG-fMRI alone was 89%, ESI alone 73% and combined EEG-fMRI/ESI 43%. Low yield has been highlighted as a limiting factor for the clinical use of EEG-fMRI. Studies report significant findings in 27% to 76% of the cases [2, 5, 13]. The improvement in the yield in our study may be explained by the population of paediatric patients studied whom typically have frequent IED and the use of topographic correlation analysis (which allowed a localisation to be achieved in the cases without IEDs).

All tests were more accurate than chance levels of correct localisation (Table 1). Both combined ESI/EEG-fMRI (92%) and ESI (82%) were more accurate than the EEG-fMRI GM localisation (50%). The results for surgical outcome prediction were consistent with the localisation results. All tests were significantly more predictive than chance levels. Both combined ESI/EEG-fMRI (91%) and ESI (83%) were more accurate than the EEG-fMRI GM localisation (50%). Importantly this surgical group of 20 included 5 patients without an MRI lesion. ESI obtained a localisation in 4/5 and in all patients it was predictive of outcome.

Combined EEG-fMRI/ESI obtained a localisation in 3/5 and in all patients it was predictive of outcome.

Comparison with previous studies

Previous studies have shown the potential of EEG-fMRI maps to localize and contribute to the EZ characterization[2, 5, 8, 13]. However, the localisation accuracy of EEG-fMRI remains poorly characterized in the literature. EEG-fMRI maps often show a multifocal pattern of significant responses and this has led to different ways of extracting a single localisation from an EEG-fMRI map. The statistic global maximum has often been used as the marker of the cluster likely to represent the EZ [5, 8]. Although the GM is an unbiased and easy method to extract a single location from a multifocal EEG-fMRI map it suffers from poor sensitivity because it is often located in regions remote from EZ. In a recent study [8] the EEG-fMRI GM was shown to have a sensitivity of 45% to localize the EZ which is in line with our findings.

The meaning and clinical significance of the often multi-focal EEG-fMRI maps of interictal epileptiform activity remains unclear, a fact closely related to the problem of defining the test's localisation result. In this study, we proposed an alternative and unbiased method to extract a single location from EEG-fMRI data by incorporating the IED information through ESI maps and assessing the concordance between them. This method relies exclusively on imaging information, avoiding the interpretation bias of viewing EEG-fMRI and ESI maps in light of clinical information. However, despite being very accurate, the yield of combined ESI and EEG-fMRI was modest (23/53) compare to EEG-fMRI (47/53) in our patient group. Given the high yield but low accuracy of the EEG-fMRI GM to define the EZ, the clinical utility of EEG-fMRI could potentially be dramatically improved by epileptic network characterisation methods that can define the EZ and regions of propagation directly from EEG-fMRI data[29]. Studies focused on comparing these results with the epileptiform activity measured invasively, including with simultaneously acquired fMRI [34, 35], may help resolve this issue.

EEG-fMRI clusters of activity and ESI maps have been shown to have both a good spatial consistency with the icEEG findings but they do not completely overlap [20]. Bagshaw et al [36] reported a mean distance of ~60 mm between the ESI and EEG-fMRI activity clusters obtained in separate sessions. In our data we found an average distance of 14 mm with a range (5 to 30) in the cases where a concordant localisation was found with EEG-fMRI and ESI. These distances and the concordance between ESI and EEG-fMRI GM are consistent with a previous study in adults [29]. This difference could suggest that each technique is more sensitive to different regions involved in the IED and may contribute to a better characterization of EZ than each map alone. However, EEG source localisation is typically considered to have a spatial accuracy of order ~1cm and there are likely to be differences in the location of the maxima of regional electrical and hemodynamic responses the latter being sensitive to the local vascular architecture. These methodological considerations could easily account for the average difference in localisation of 14mm found here. There

are a number of methodological choices that could influence the accuracy of the ESI results. A greater EEG density (above the 64 channels used here) may improve the spatial accuracy of ESI [37, 38]. We used a Spherical Head Model with Anatomical Constraints (SMAC) based on a 3-shell spherical realistic head model and the patient's individual MRI spherical head model, this is an active area of research and more advanced and specific models may also improve accuracy [38] . These methodological choices were motivated by our desire to make a comparison to the largest study of the application of ESI to presurgical epilepsy evaluation in the literature [37] and so we therefore followed the same approach.

ESI was shown to accurately map the generators of IED from data obtained during an EEG-fMRI recording in our paediatric population, providing useful predictive information for the presurgical assessment. The sensitivity of ESI alone to localise the EZ was 82% which replicates the results in a previous study, which examined a mixed cohort of adults and children using EEG data from outside the scanner[16]. ESI is therefore a technique that can provide a relatively low cost minimally invasive test with high accuracy in the context of evaluation for paediatric epilepsy surgery. However, its accuracy may be more limited in some cases such as those with deep sources, or in patients with brain and skull abnormalities. In our sample, there were 6 cases in whom ESI was inconsistent with the MRI lesion. Four of them were patients with deep lesions and one patient had undergone previous surgery.

To determine test sensitivity and their reliability we used a Bayesian approach. This allowed the incorporation of prior information (where available) to increase the confidence in our results. For ESI and EEG-fMRI-GM the priors on the sensitivity were very consistent with the data from the current study and therefore their incorporation had little effect on the sensitivity but reduced the credible interval (crucially allowing for more accurate population level inference). For the combined EEG-fMRI/ESI the uninformative prior reduces the sensitivity estimate (reflecting our uncertainty in this novel methodology due to low numbers). Using this approach, future studies can readily update these numbers to further refine these sensitivity estimates by using our posterior distributions as priors in their work.

Clinical value

The aim of presurgical evaluation is to identify a clear hypothesis for the EZ that can be confirmed by intracranial recording or allows for surgery to be offered with an appropriate understanding of risk-benefit. In patients that have an MRI lesion consistent with electro-clinical information this is often achieved. However, for patients without an MRI lesion it becomes difficult to formulate a spatially constrained hypothesis. PET and SPECT can be used to formulate a spatial hypothesis [39], however the spatial accuracy of these techniques is poor. In this study, we have shown that a combined EEG-fMRI & ESI result from a single data set is highly localizing and predictive of surgical outcome with or without an MRI lesion. Furthermore, the localisation provided by these tests (typically at the sublobar level) is more

spatially accurate than most of the current non-invasive presurgical test (EEG, PET & SPECT) which are used to localize the EZ in patients with no MRI lesion.

Limitations

This study is limited by the numbers in the subgroup of patients in whom the validation of the localisation results could be carried out (29/53). This represents a potential (but unavoidable) bias, because the patients in whom an EZ is well characterised may not fully represent the sample. We included a group of 23 MR negative patients that have a poorer likelihood of having a well-defined EZ, and therefore surgical outcome data. This choice was necessitated by the need for an assessment of the localisation tests accuracy in this group. A combined EEG-fMRI/ESI localisation was found in 12/23 MRI negative patients and outcome was predicted in all 3 whom had surgery. Our results therefore strongly motivate a larger study of combined EEG-fMRI and ESI in MRI negative patients with validation based on intracranial EEG or surgery.

Patients with a well-defined cortical MRI abnormality concordant with electro-clinical information are unlikely to benefit from EEG-fMRI given its cost. In these cases, based on our data, ESI represents an additional relatively low-cost test with a good sensitivity in children with frequent IEDs. However, patients without an MRI visible abnormality, a deep lying or extensive MRI abnormality, and/or prior surgery are likely to benefit from combined EEG-fMRI and ESI.

Acknowledgements:

This project was funded by Action Medical Research grant number SP4646. D.C. is supported by the Engineering and Physical Sciences Research Council grant EP/M001393/1. E .S. and T.T. are supported by the James Lewis Foundation (via Great Ormond Street Hospital Children's Charity) the Child Health Research Appeal Trust. E.S. is funded by University College London Overseas Research Scholarship. T.T. is founded by University College London IMPACT. S.P. is supported by NIHR Biomedical Research founding. SV is supported by Swiss National Science Foundation grant SNF 141165 and the Gertrude von Meissner Foundation. The Cartool software (http://brainmapping.unige.ch/cartool) has been programmed by Denis Brunet from the Functional Brain Mapping Laboratory, Geneva, and is supported by the Center for Biomedical Imaging (CIBM) of Geneva and Lausanne, Switzerland. We acknowledge the support of the National Institute of Health Research Great Ormond Street Hospital Biomedical Research Centre in performing this work.

Acknowledgements:

This project was funded by Action Medical Research grant number SP4646. D.C. is supported by the Engineering and Physical Sciences Research Council grant EP/M001393/1. E.S. and T.T. are supported by the James Lewis Foundation (via Great Ormond Street Hospital Children's Charity) the Child Health Research Appeal Trust. E.S. is funded by University College London Overseas Research Scholarship. T.T. is founded by University College London IMPACT. S.P. is supported by NIHR Biomedical Research founding. SV is supported by Swiss National Science Foundation grant SNF 141165 and the Gertrude von Meissner Foundation. The Cartool software (http://brainmapping.unige.ch/cartool) has been programmed by Denis Brunet from the Functional Brain Mapping Laboratory, Geneva, and is supported by the Center for Biomedical Imaging (CIBM) of Geneva and Lausanne, Switzerland. We acknowledge the support of the National Institute of Health Research Great Ormond Street Hospital Biomedical Research Centre in performing this work.

We are grateful to Tina Banks who acquired the MRI data and to all the patients that participate in this study for their generosity and to the clinicians and neurophysiologist in the epilepsy unit at Great Ormond Street Hospital.

Authors contributions:

The authors in this work have contributed in the following way: M.C. and D.C. and T.T contributed to conceiving and designed the experiments, M.C, T.T, E.S, S.P, D.K, K.S, C.W, F.G and D.C. contributed to analyzing the data. M.C, T.T, D.C, S.V, L.L, R.P, C.C and H.C. contributed to drafting the text and preparing the figures.

Potential Conflicts of Interest

D.C. receives in kind support from Brain Products (Gmbh, Gilching, Germany) as part of a grant (Engineering and physical sciences research council EP/M001393/1). Brain products manufactures the EEG system used in this study. The remaining authors have no conflict of interest.

BIBLIOGRAPHY

1. Skirrow C, Cross JH, Cormack F, Harkness W, Vargha-Khadem F, Baldeweg T. Long-term intellectual outcome after temporal lobe surgery in childhood. Neurology. 2011 Apr 12;76(15):1330-7.
2. Salek-Haddadi A, Diehl B, Hamandi K, et al. Hemodynamic correlates of epileptiform discharges: an EEG-fMRI study of 63 patients with focal epilepsy. Brain Res. 2006 May 9;1088(1):148-66.
3. Zijlmans M, Huiskamp G, Hersevoort M, Seppenwoolde JH, van Huffelen AC, Leijten FS. EEG-fMRI in the preoperative work-up for epilepsy surgery. Brain : a journal of neurology. 2007 Sep;130(Pt 9):2343-53.
4. Chaudhary UJ, Carmichael DW, Rodionov R, et al. Mapping preictal and ictal haemodynamic networks using video-electroencephalography and functional imaging. Brain. 2012 Dec;135(Pt 12):3645-63.
5. Pittau F, Dubeau F, Gotman J. Contribution of EEG/fMRI to the definition of the epileptic focus. Neurology. 2012 May 8;78(19):1479-87.
6. van Houdt PJ, de Munck JC, Leijten FS, et al. EEG-fMRI correlation patterns in the presurgical evaluation of focal epilepsy: a comparison with electrocorticographic data and surgical outcome measures. NeuroImage. 2013 Jul 15;75:238-48.
7. Thornton R, Vulliemoz S, Rodionov R, et al. Epileptic networks in focal cortical dysplasia revealed using electroencephalography-functional magnetic resonance imaging. Ann Neurol. 2011 Nov;70(5):822-37.
8. An D, Fahoum F, Hall J, Olivier A, Gotman J, Dubeau F. Electroencephalography/functional magnetic resonance imaging responses help predict surgical outcome in focal epilepsy. Epilepsia. 2013 Dec;54(12):2184-94.
9. Laufs H. Functional imaging of seizures and epilepsy: evolution from zones to networks. Current opinion in neurology. 2012 Apr;25(2):194-200.
10. Terry JR, Benjamin O, Richardson MP. Seizure generation: the role of nodes and networks. Epilepsia. 2012 Sep;53(9):e166-9.

11. Vulliemoz S, Rodionov R, Carmichael DW, et al. Continuous EEG source imaging enhances analysis of EEG-fMRI in focal epilepsy. Neuroimage. 2010 Feb 15;49(4):3219-29.
12. Tousseyn S, Dupont P, Goffin K, Sunaert S, Van Paesschen W. Correspondence between large-scale ictal and interictal epileptic networks revealed by single photon emission computed tomography (SPECT) and electroencephalography (EEG)-functional magnetic resonance imaging (fMRI). Epilepsia. 2015 Mar;56(3):382-92.
13. Thornton R, Laufs H, Rodionov R, et al. EEG correlated functional MRI and postoperative outcome in focal epilepsy. J Neurol Neurosurg Psychiatry. 2010 Aug;81(8):922-7.
14. Centeno M, Tierney TM, Perani S, et al. Optimising EEG-fMRI for Localisation of Focal Epilepsy in Children. PloS one. 2016;11(2):e0149048.
15. Grouiller F, Thornton RC, Groening K, et al. With or without spikes: localisation of focal epileptic activity by simultaneous electroencephalography and functional magnetic resonance imaging. Brain : a journal of neurology. 2011 Oct;134(Pt 10):2867-86.
16. Brodbeck V, Spinelli L, Lascano AM, et al. Electroencephalographic source imaging: a prospective study of 152 operated epileptic patients. Brain : a journal of neurology. 2011 Oct;134(Pt 10):2887-97.
17. Russo A, Jayakar P, Lallas M, et al. The diagnostic utility of 3D electroencephalography source imaging in pediatric epilepsy surgery. Epilepsia. 2016 Jan;57(1):24-31.
18. Merlet I, Gotman J. Dipole modeling of scalp electroencephalogram epileptic discharges: correlation with intracerebral fields. Clinical neurophysiology : official journal of the International Federation of Clinical Neurophysiology. 2001 Mar;112(3):414-30.
19. Benar CG, Gotman J. Modeling of post-surgical brain and skull defects in the EEG inverse problem with the boundary element method. Clinical neurophysiology : official journal of the International Federation of Clinical Neurophysiology. 2002 Jan;113(1):48-56.
20. Benar CG, Grova C, Kobayashi E, et al. EEG-fMRI of epileptic spikes: concordance with EEG source localization and intracranial EEG. NeuroImage. 2006 May 1;30(4):1161-70.
21. Grova C, Daunizeau J, Kobayashi E, et al. Concordance between distributed EEG source localization and simultaneous EEG-fMRI studies of epileptic spikes. NeuroImage. 2008 Jan 15;39(2):755-74.
22. Elshoff L, Groening K, Grouiller F, et al. The value of EEG-fMRI and EEG source analysis in the presurgical setup of children with refractory focal epilepsy. Epilepsia. 2012 Sep;53(9):1597-606.
23. Wieser HG, Blume WT, Fish D, et al. ILAE Commission Report. Proposal for a new classification of outcome with respect to epileptic seizures following epilepsy surgery. Epilepsia. 2001 Feb;42(2):282-6.
24. Tierney TM, Weiss-Croft LJ, Centeno M, et al. FIACH: A biophysical model for automatic retrospective noise control in fMRI. NeuroImage. 2016 Jan 1;124(Pt A):1009-20.
25. Jacobs J, Kobayashi E, Boor R, et al. Hemodynamic responses to interictal epileptiform discharges in children with symptomatic epilepsy. Epilepsia. 2007 Nov;48(11):2068-78.
26. Laufs H, Hamandi K, Salek-Haddadi A, Kleinschmidt AK, Duncan JS, Lemieux L. Temporal lobe interictal epileptic discharges affect cerebral activity in "default mode" brain regions. Human brain mapping. 2007 Oct;28(10):1023-32.
27. Michel CM, Murray MM, Lantz G, Gonzalez S, Spinelli L, Grave de Peralta R. EEG source imaging. Clinical neurophysiology : official journal of the International Federation of Clinical Neurophysiology. 2004 Oct;115(10):2195-222.
28. Lopes da Silva FH. A critical review of clinical applications of topographic mapping of brain potentials. Journal of clinical neurophysiology : official publication of the American Electroencephalographic Society. 1990 Oct;7(4):535-51.
29. Vulliemoz S, Thornton R, Rodionov R, et al. The spatio-temporal mapping of epileptic networks: combination of EEG-fMRI and EEG source imaging. NeuroImage. 2009 Jul 1;46(3):834-43.
30. Knowlton RC, Elgavish RA, Bartolucci A, et al. Functional imaging: II. Prediction of epilepsy surgery outcome. Annals of neurology. 2008 Jul;64(1):35-41.

31. Gelman A. Bayesian data analysis. London: Chapman & Hall; 1995.
32. Canty A, Ripley B. boot: Bootstrap R (S-Plus) Functions. R package version 1.3-18. 2016.
33. R-Core-team. R: A Language and Environment for Statistical Computing. R Foundation for Statistical Computing , Vienna, Austria. ISBN 3-900051-07-0, URL http://www.R-Project.org/. 2015.
34. Vulliemoz S, Carmichael DW, Rosenkranz K, et al. Simultaneous intracranial EEG and fMRI of interictal epileptic discharges in humans. NeuroImage. 2011 Jan 1;54(1):182-90.
35. Carmichael DW, Vulliemoz S, Rodionov R, Thornton JS, McEvoy AW, Lemieux L. Simultaneous intracranial EEG-fMRI in humans: protocol considerations and data quality. Neuroimage. 2012 Oct 15;63(1):301-9.
36. Bagshaw AP, Kobayashi E, Dubeau F, Pike GB, Gotman J. Correspondence between EEG-fMRI and EEG dipole localisation of interictal discharges in focal epilepsy. NeuroImage. 2006 Apr 1;30(2):417-25.
37. Brodbeck V, Spinelli L, Lascano AM, et al. Electroencephalographic source imaging: a prospective study of 152 operated epileptic patients. Brain. 2011 10/2011;134(Pt 10):2887-97.
38. Kaiboriboon K, Luders HO, Hamaneh M, Turnbull J, Lhatoo SD. EEG source imaging in epilepsy--practicalities and pitfalls. Nature reviews Neurology. 2012 Sep;8(9):498-507.
39. Duncan JS, Winston GP, Koepp MJ, Ourselin S. Brain imaging in the assessment for epilepsy surgery. The Lancet Neurology. 2016 Apr;15(4):420-33.

FIGURE LEGENDS

Figure 1: Localisation extraction procedure

From left to right; EEG-fMRI data is used to obtain a map for EEG-fMRI and ESI. For each of these individual maps a single localisation is selected: for the EEG-fMRI the global maxima is selected and for the ESI the maxima in the map from the 50% rising phase of the IED is selected. For the combined test the localisation is derived from the spatial conjunction of both maps. Where the maps are concordant the localisation is the region encompassing the ESI max and the closest significant EEG-fMRI cluster located in same sublobe. When the maps are discordant cases no combined localisation is extracted.

Figure 2: Validation of individual and combined EEG-fMRI and ESI maps

The localisations derived from the single and combined test were validated by:

1) Calculating localisation accuracy in those patients with a well characterized EZ. For each localisation method its accuracy was classified as a true positive (TP) if it was located in the presumed EZ (top row) or False positive (FP) if it was not;

2) Calculating the prediction accuracy for seizure outcome in all patients who underwent surgery (bottom row). Here a true positive (TP) was a localisation within

the resection margins and good outcome; a false negative (FN) was a localisation within the resection margins and poor outcome; true (TN) and false negatives (FN) were a localisation that was not within the resection margins and a poor or good outcome respectively.

Figure 3: Summary flowchart

The number of significant results for each of the test individually and in combination is summarised in for the MRI negative and MRI lesion patients respectively. The diagram shows the number patients with a combined EEG-fMRI/ESI result that were validated by surgical outcome for MRI lesion and MRI negative patients.

Table Legends

Table 1: Yield, localisation accuracy and prediction accuracy

Test yield is calculated as the number of subjects in whom a significant map was obtained.

Localisation accuracy was calculated in those patients with well localized epileptogenic zone (EZ), and surgical prediction in those patients who underwent surgical resection. n is the number of subjects where the test provided a result. The current study summary row gives the number of true positives (TP), false positives (FP), true negatives (TN) and false negatives (FN) . The test sensitivity is, given a result, the likelihood it was correct; α and β are the hyperparameters of the beta distribution. Prior hyperparameters are based on the results of previous studies where available or are set to both equal 1 where there is no prior information.

Supplementary Table1: Clinical data.

Presumed epileptogenic zone (EZ) is the region where the EZ was located after non-invasive test. In those patients with well characterized EZ (presence of MRI lesion or good surgical outcome) the relative volume of EZ was estimated by the following process. When the resected cavity or MRI lesion was defined as being at a hemisphere level a volume of 0.5 was assigned, lobar level lesions or resections were assigned a relative brain volume of 0.1 for occipital, temporal and parietal lobes and 0.2 for the frontal lobe. For sublobar lesions or resections the volume was estimated by expert visual assignment of the AAL atlas regions involved (M.C.). The relative volume was then calculated as a sum of AAL regions relative volume. One patient had a hypothalamic haematoma and therefore a relative volume of 0.03 was used. Note that this approach was used to provide a maximum bound on the EZ volume and therefore a conservative statistical assessment of localisation probabilities.

Abbreviations: m=male f=female L=left R=right TL=temporal lobe No=no MRI lesion DNET=Dysembryoplastic neuro epithelial tumour FCD=focal cortical dysplasia. AED=

antiepileptic drugs; VPA=valproate TPM=topiramate CBZ=carbamazepine LMT=Lamotrigine CBZ =Clobazam OXC=Oxcarbazepine LVT=Levetiracetam PHE=Phenytoin RUF=Rufinamide PPN=Perampanel VGB=Vigabatrin AZAT=Azathioprine
Surgery outcome for the 20 patients who underwent surgery is classified using the ILAE classification.

Supplementary Table 2: EEG-fMRI and ESI results: Availability and localisation of EEG-fMRI and ESI results for each subject.

Significant results for EEG-fMRI and ESI maps are indicated with a ✓. No available results for the test are indicated with X. The concordance column shows whether EEG-fMRI and ESI maps where concordant (=C) or discordant (=D) for those cases that have both maps. The localisation of EZ column contains the cases in whom the localisation of each single test and combine test correctly identifies the ER (TP=true positive) or not (FP=false positive). The surgery prediction column displays the results for the localisation of individual and combined EEG-fMRI and ESI correctly predict surgery outcome (TP=true positive=localisation included in resection+good outcome); (FP=false positive=localisation resected and poor outcome); (TN-true negative=localisation not resected+poor outcome); (FN=false negative=localisation not resected+good outcome).

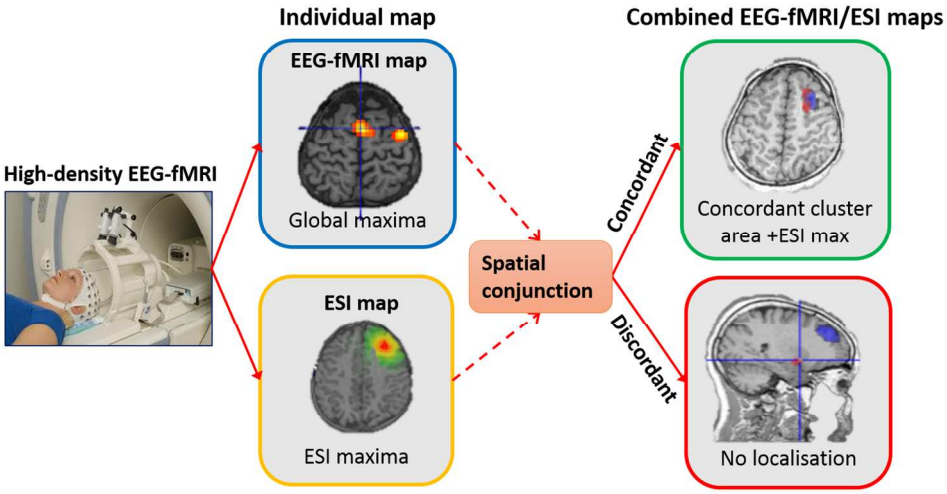

Figure 1: Localisation extraction procedure
From left to right; EEG-fMRI data is used to obtain a map for EEG-fMRI and ESI. For each of these individual maps a single localisation is selected: for the EEG-fMRI the global maxima is selected and for the ESI the maxima in the map from the 50% rising phase of the IED is selected. For the combined test the localisation is derived from the spatial conjunction of both maps. Where the maps are concordant the localisation is the region encompassing the ESI max and the closest significant EEG-fMRI cluster located in same sublobe. When the maps are discordant cases no combined localisation is extracted.

170x92mm (300 x 300 DPI)

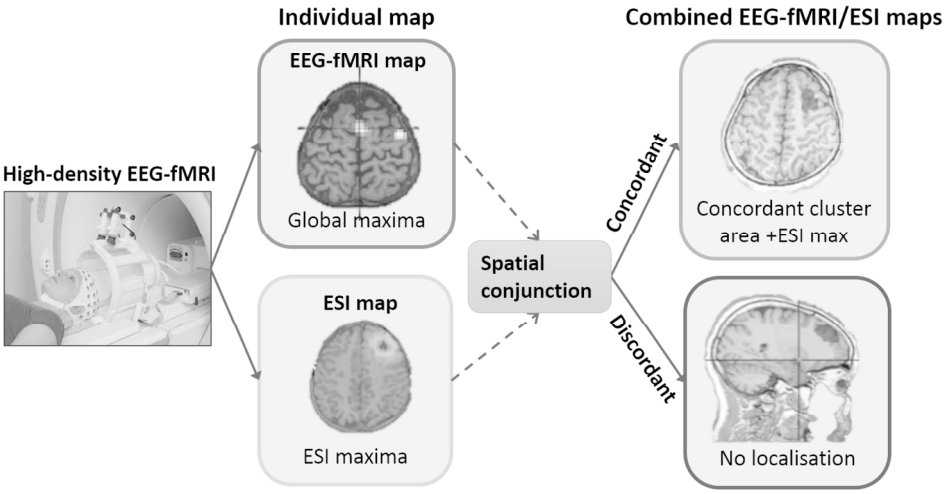

Figure 1: Localisation extraction procedure
From left to right; EEG-fMRI data is used to obtain a map for EEG-fMRI and ESI. For each of these individual maps a single localisation is selected: for the EEG-fMRI the global maxima is selected and for the ESI the maxima in the map from the 50% rising phase of the IED is selected. For the combined test the localisation is derived from the spatial conjunction of both maps. Where the maps are concordant the localisation is the region encompassing the ESI max and the closest significant EEG-fMRI cluster located in same sublobe. When the maps are discordant cases no combined localisation is extracted.

170x92mm (300 x 300 DPI)

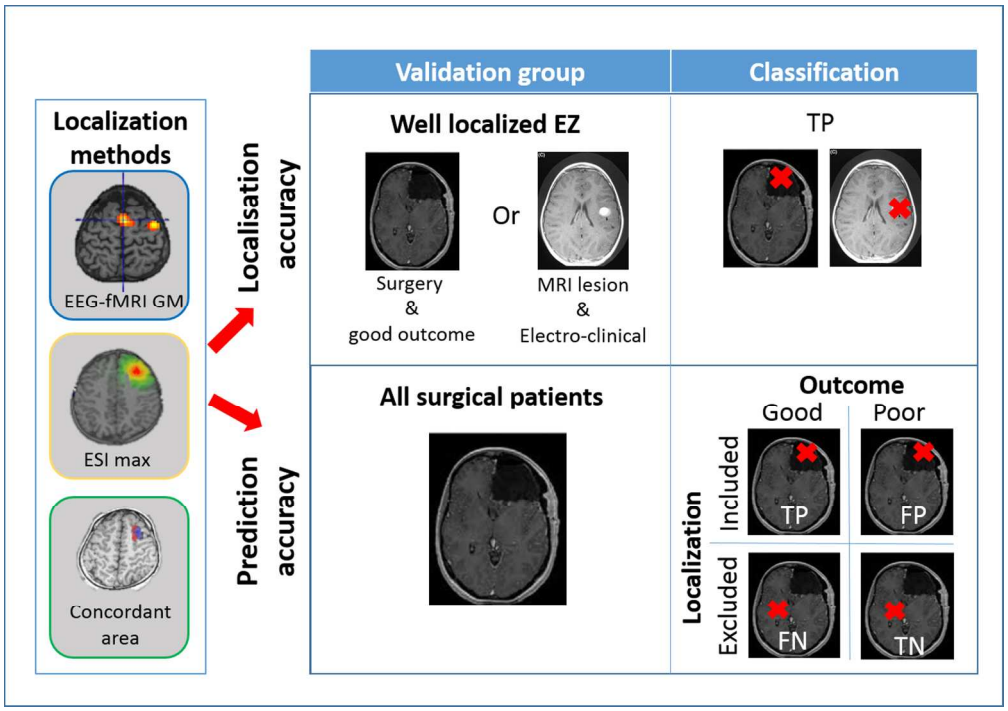

Figure 2: Validation of individual and combined EEG-fMRI and ESI maps
The localisations derived from the single and combined test were validated by:
1) Calculating localisation accuracy in those patients with a well characterized EZ. For each localisation method its accuracy was classified as a true positive (TP) if it was located in the presumed EZ (top row) or False positive (FP) if it was not;
2) Calculating the prediction accuracy for seizure outcome in all patients who underwent surgery (bottom row). Here a true positive (TP) was a localisation within the resection margins and good outcome; a false negative (FN) was a localisation within the resection margins and poor outcome; true (TN) and false negatives (FN) were a localisation that was not within the resection margins and a poor or good outcome respectively.

170x119mm (300 x 300 DPI)

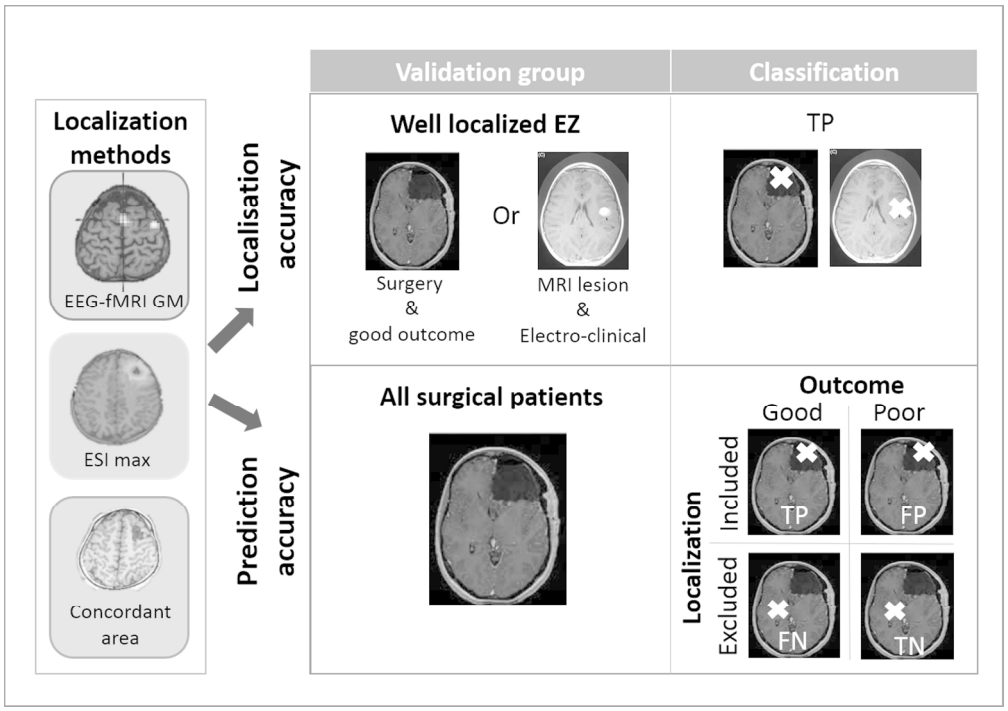

Figure 2: Validation of individual and combined EEG-fMRI and ESI maps
The localisations derived from the single and combined test were validated by:
1) Calculating localisation accuracy in those patients with a well characterized EZ. For each localisation method its accuracy was classified as a true positive (TP) if it was located in the presumed EZ (top row) or False positive (FP) if it was not;
2) Calculating the prediction accuracy for seizure outcome in all patients who underwent surgery (bottom row). Here a true positive (TP) was a localisation within the resection margins and good outcome; a false negative (FN) was a localisation within the resection margins and poor outcome; true (TN) and false negatives (FN) were a localisation that was not within the resection margins and a poor or good outcome respectively.

170x119mm (300 x 300 DPI)

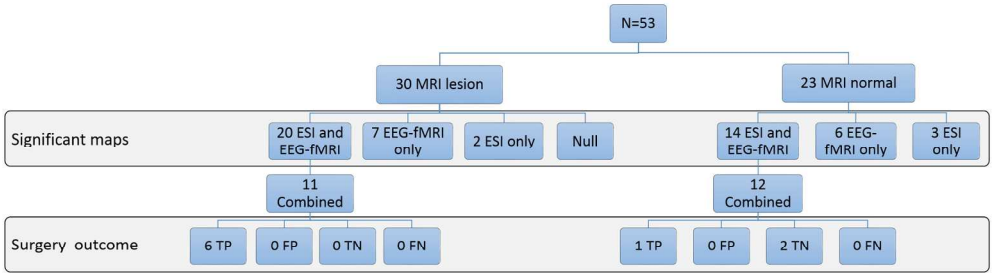

Figure 3: Summary flowchart
The number of significant results for each of the test individually and in combination is summarised in for the MRI negative and MRI lesion patients respectively. The diagram shows the number patients with a combined EEG-fMRI/ESI result that were validated by surgical outcome for MRI lesion and MRI negative patients.

170x67mm (300 x 300 DPI)

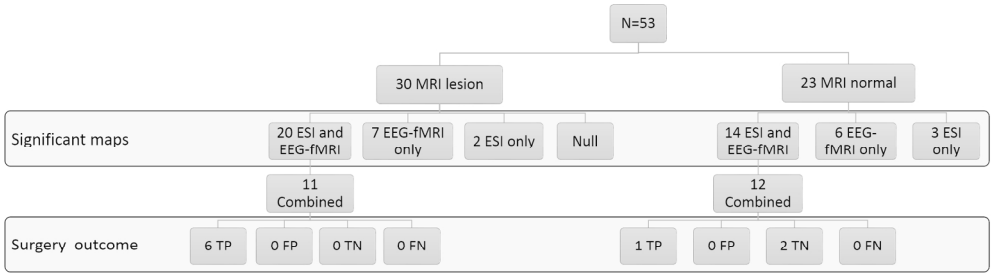

Figure 3: Summary flowchart
The number of significant results for each of the test individually and in combination is summarised in for the MRI negative and MRI lesion patients respectively. The diagram shows the number patients with a combined EEG-fMRI/ESI result that were validated by surgical outcome for MRI lesion and MRI negative patients.

170x67mm (300 x 300 DPI)

ID	AGE	GENDER	MRI LESION	PRESUMED EZ	RELATIVE VOLUME EZ	AED	SURGERY	TYPE OF SURGERY	OUTCOME (ILAE)
#1	8	f	Tuberosclerosis. L temporal prominent tuber	L temporo-parietal	0.015	ZNS	N		
#2	14	f	No	L Frontal	0.018	LAC, LVT	Y	Frontal tailored resection	5
#3	11	m	Hypothalamic hamartoma	L temporal	0.03	LVT	N		
#4	15	m	No	L posterior quadrant		CBZ	N		
#5	11	f	No	R F-T Junction		LAC, GBP, CLBZ	N		
#6	17	m	R parietal FCD	R parietal	0.034	LVT, CLBZ, VPA	N		
#7	15	m	No	R Frontal medial/lateral	0.018	CBZ	Y	Frontal tailored resection	1
#8	17	f	L Temporal FCD	L temporal posterior	0.091	LVT	Y	L temporal lobectomy	1
#9	11	f	Perinatal L hemisphere cortical atrophy	L hemisphere possible central region	0.5	OXC	N		
#10	14	f	R temporal FCD 2B	R temporal	0.075	LVT, TPM	Y	R Temporal lobectomy	1
#11	11	f	No	R Fronto-temporal		CBZ, LMT	N		
#12	11	m	No	R F-T		CBM, TPM	N		
#13	10	f	R frontal pole FCD	R fronto-polar	0.009	OXC	Y	Frontal tailored resection	1

#14	12	m	Skull malformation/ R hemispheric cortical atrophy	R hemisphere possibly multifocal	0.5	VPA	N		
#15	17	f	No	R frontal		LTG LEV	N		
#16	16	f	No	L frontal		VPA CBZ	N		
#17	11	f	No	L frontal (Medial frontal cingulum/frontal operculum)		OXC, CLBZ VGB	N		
#18	17	f	L posterior temporal astrocytoma. Previous resection	L temporal lobe	0.013	TPM OXC	N		
#19	14	m	Autoinmune L hemisphere cortical atrophy	L hemisphere. Medila temporal semiology	0.5	AZIA, VPA MDZ	Y	Hemispherectomy	4
#20	16	f	L insular FCD	L insula-deep	0.004	TPM CBZ	N		
#21	18	m	R precuneus FCD 2A	R precuneus	0.013	LAC LMT PGB TPM	Y	Parietal resection	5
#22	11	m	No	R frontal		CBZ	N		
#23	11	m	No	R frontal		LVT VPA	N		
#24	16	f	L T-P-O polymicrogyria /Unspecific cortical atrophy	Deep L hemisphere lesion	0.3	LVT CLNZ	N		
#25	15	m	No	T-P-O/ temporal medial	0.091	LMT ZNS	Y	Temporal resection	5
#26	15	m	No	L temporal		OXC LEV	N		
#27	17	f	No	Frontal		OXC	N		

#28	8	f	L middle cerebral artery stroke	L frontal	0.2	VPA LVT ETHx	Y	Anterior quadrant disconnection	4
#29	17	m	L post-central FCD	Parietal	0.013	LVT	Y		4
#30	16	f	L perisylvian polymicogyria	L perysilvian	0.071	PPN	Y	Partial frontal resection	4
#31	16	m	No	R frontal		CBZ LVT	N		
#32	11	m	L choroid plexus papilloma. L posterior quadrant atrophy secondary to radiotherapy	L posterior quadrant	0.2	VPA CBZ PPN	N		
#33	13	m	L middle frontal gyrus FCD	R frontal	0.017	OXC CLBZ	Y	Partial frontal resection	1
#34	10	f	No	L frontal		LVT CBZ	N		
#35	10	m	No	R T-P-O		OXC	N		
#36	14	m	L middle cerebral artery stroke	L occipital	0.5	OXC GBP	Y	Hemispherotomy	1
#37	17	m	No	Unknown		LVT OXC CLBZ	N		
#38	17	m	L occipital atrophy. Iquemic perinatal insult	R occipital	0.1	OXC LMT LVT	N		
#39	13	m	L T-P-O cortical atrophy perinatal	L occipital	0.212	CBZ TPM CLBZ	Y	Posterior quadrant disconnection	4
#40	18	f	R frontal FCD	R frontal	0.042	LMT	Y	Partial frontal resection	2
#41	17	f	Bilateral oribito-frontal	Bilateral orbito-frontal	0.009	LVT VPA	N		

			polymicrogyria						
#42	17	m	R T-P-O junction postusurgery residual FCDi	Fronto-parietal	0.007	OXC TPM RUF	N		
#43	15	m	No	Frontal medial		VPA LAC CLBZ	N		
#44	11	f	No	R parietal	0.019	OXC PHE CLBZ	Y	Partial parietal resection	5
#45	17	m	No	Frontal lobe		LVT LAC	N		
#46	18	m	R inferior parietal residual postsurgical DNET	R parietal	0.018	LAC LMT	N		
#47	11	f	R parietal FCD	R parietal	0.021	OXC CLBZ VPA	Y	Partial parietal resection	1
#48	13	f	R amygdala DNET	R medial TL	0.04	TPM	Y	Anterior temporal lobe resection	1
#49	12	m	Bilateral perisylvian polymicrogyria	R fronto-parietal junction	0.048	VPA LVT CBZ CBZ	N		
#50	17	f	No	L frontal midline	0.018	VPA	Y	Partial frontal lobe resection	1
#51	13	f	L inferior frontal FCD	L frontal	0.025	VPA	N		
#52	15	f	R posterior cingulate DNET	R medial parietal	0.002	LVT LMT	Y	R posterior cingulate resection	1
#53	7	m	No	L frontal		LVT OXC CLBZ	N		

		Chance Level	EEG-FMRI_GM	ESI	Combined Method
Yield n=53	**Test Yield**		**47/53 (89%)**	**39/53 (73%)**	**23/53 (43%)**
Localisation n=29	*n*	29	26	22	12
	Current study-summary		TP=11, FP=15	TP=17, FP=5	TP=11, FP=1
	Current study	-	α=11, b=15	α=17, β=5	α=11, β=1
	Prior Hyperparameters	-	α=14, β=10	α=45, β=9	α=1, β=1
	Posterior Distribution	-	α=25, β=25	α=62, β=14	α=12, β=1
	Sensitivity	**11%**	**25/50 (50%)**	**62/76 (82%)**	**12/13 (92%)**
	95% Credible Interval	6%-17%	36 - 64%	72% - 89%	64% - 98%
Prediction n=20	*n*	20	20	16	9
	Current study-summary		TP=3, TN=5, FP=1, FN=11	TP=10, TN=3, FP=1, FN=2	TP=7, TN=2, FP=0, FN=0
	Current study	-	α=8, β=12	α=13, β=3	α=9, β=0
	Prior Hyperparameters	-	α=14, β=10	α=45, β=9	α=1, β=1
	Posterior Distribution	-	α=22, β=22	α=58, β=12	α=10, β=1
	Sensitivity	**10%**	**22/44 (50%)**	**58/70 (83%)**	**10/11 (91%)**
	95% Credible Interval	4%-17%	36 - 65%	73% - 91%	69% - 100%

Table 1: Yield, localisation accuracy and prediction accuracy